Hindawi
Complexity
Volume 2020, Article ID 9260823, 12 pages
https://doi.org/10.1155/2020/9260823

Research Article

A Novel Megastable Hamiltonian System with Infinite Hyperbolic and Nonhyperbolic Equilibria

Gervais Dolvis Leutcho,[1,2] Theophile Fonzin Fozin,[3] Alexis Nguomkam Negou,[1,4] Zeric Tabekoueng Njitacke,[5] Viet-Thanh Pham,[6,7] Jacques Kengne,[4] and Sajad Jafari[8]

[1]*Research Unit of Laboratory of Condensed Matter, Electronics and Signal Processing (UR-MACETS) Department of Physics, Faculty of Sciences, University of Dschang, P.O. Box 67, Dschang, Cameroon*
[2]*Department of Physics, Faculty of Sciences, University of Mons, P.O. Box 7000, Mons, Belgium*
[3]*Department of Electrical and Electronic Engineering, Faculty of Engineering and Technology (FET), University of Buea, P.O. Box 63, Buea, Cameroon*
[4]*Research Unit of Laboratory of Automation and Applied Computer (LAIA), Electrical Engineering Department of IUT-FV, University of Dschang, P.O. Box 134, Bandjoun, Cameroon*
[5]*Department of Electrical and Electronic Engineering, College of Technology (COT), University of Buea, P.O. Box 63, Buea, Cameroon*
[6]*Faculty of Electrical and Electronic Engineering, Phenikaa Institute for Advanced Study (PIAS), Phenikaa University, Yen Nghia, Ha Dong district, Hanoi 100000, Vietnam*
[7]*Phenikaa Research and Technology Institute (PRATI), A&A Green Phoenix Group, 167 Hoang Ngan, Hanoi 100000, Vietnam*
[8]*Biomedical Engineering Department, Amirkabir University of Technology, Tehran 15875-4413, Iran*

Correspondence should be addressed to Gervais Dolvis Leutcho; leutchoeinstein@yahoo.com

Received 29 April 2020; Revised 10 August 2020; Accepted 8 September 2020; Published 28 September 2020

Academic Editor: Carlos Aguilar-Ibanez

The dimension of the conservative chaotic systems is an integer and equals the system dimension, which brings about a better ergodic property and thus have potentials in engineering application than the dissipative systems. This paper investigates the phenomenon of megastability in a unique and simple conservative oscillator with infinite of hyperbolic and nonhyperbolic equilibria. Using traditional nonlinear analysis tools, we found that the introduced oscillator possesses an invariable energy and displays either self-excited or hidden dynamics depending on the stability of its equilibria. Besides, the conservative nature of the new system is validated using theoretical measurement. Furthermore, an analog simulator of the oscillator is built and simulated in the PSpice environment to confirm that the previous results were not artifacts.

1. Introduction

Considerable efforts have been made recently by several authors in designing chaotic systems with striking features linked to their equilibria [1–7]. These dynamical systems include some with no equilibrium point [8], stable equilibria [1, 9–11], infinite equilibria [12–17], and unstable equilibria [2, 18, 19]. The latter belongs to self-excited nonlinear dynamical systems, while the formers are new and classified as systems with hidden attractors [20–22]. Several systems with hidden attractors are linked to multistability which refers to the coexistence of multiple attractors for the same group of parameters [23–25]. Indeed, a system may approach different stable states starting from different initial values. When the system basin of initial conditions is associated with unstable equilibrium points, one may find countable coexisting attractors. However, when the system has a great deal of the coexisting attractors, the phenomenon is defined as extreme multistability. Despite the intensive efforts in reporting systems with hidden attractors, most of the

attention so far was oriented only on structure and characteristic of their equilibria [26], while other important specificities including shape and topology of the strange attractors were rarely considered. Few examples are chaotic systems with varying symmetry [27], chaotic systems with conditional symmetry [28–31], multiscroll attractors [32–34], attractor growing [35, 36], algebraically simple equations [37], and nested megastable attractors [38–45].

Now in forefront of investigations, megastable systems are a special class of multistable systems with nested attractors [26]. First reported by Sprott and coauthors in [26], such systems are now widely investigated [38–45]. Although the phenomenon of megastability in chaotic systems was up to date linked to additional external excitation [46, 47], the recent work by Kathikeyan and colleagues demonstrates that the above condition is not mandatory [48]. However, very few megastable systems reported so far are conservative. Conservative chaotic flow is a category of incompressible chaos usually generated from dynamical systems without dissipation. Based on a long history and formalism from Euler, Lagrange Hamilton, and Jacobi [49], the main characteristic of such systems is that they do not have attractors because their phase space volumes are conserved [50]. However, such systems can exhibit complicated dynamical behaviors including chaos [37]. The dimension of the conservative chaotic systems is an integer and equals the system dimension, which brings about a better ergodic property than the dissipative system. Consequently, the probability distribution associated with conservative chaos is relatively flat like the uniform distribution of white noise, whereas dissipative chaos has either a single peak or multiple peaks, from which the main frequency characteristics can be identified. Clearly, the information encrypted based on the former can be decrypted or attacked based on frequency reconstruction [51] while the latter (conservative system) is adapted [37]. Therefore, with both having the same bandwidths, the conservative chaotic system is more suitable as a pseudorandom number generator than the dissipative chaotic system. Owing to the importance of conservative/Hamiltonian systems in the mechanical domain, we propose in this work an extremely simple megastable Hamiltonian system with its circuitry implementation.

It is observed from Table 1 that no 2D conservative system with infinite hyperbolic and nonhyperbolic equilibria and few terms (i.e., three) was reported in the literature. Also, Table 2 highlights the megastability (i.e., coexistence of infinite countable attractors) property of some simple conservative systems proposed within this work. To the best of the authors' knowledge, no such simple conservative 2D system with both megastability and multistability was yet reported in the relevant literature so far and thus deserves dissemination.

The organization of this paper is as follows. Section 2 deals with the introduction and description of the new conservative megastable system. Preliminary analysis including investigations of steady states and their nature is presented. Then, Section 3 is dedicated to the conservative feature/property of the new system with two different methods, namely, divergence and Hamiltonian. In Section 4, numerical investigations of the forced derivative of the newly introduced system are performed based on well-known nonlinear dynamical tools including bifurcation diagrams, Lyapunov exponents, and phase portraits. In Section 5, an experimental study is carried out. The results of the corresponding electronic circuit implemented in the PSpice simulation environment show a good agreement with obtained numerical investigations. The last section concludes the paper.

2. The New Simple Conservative Megastable Oscillator

Consider the following two-dimensional (2D) dissipative nonlinear oscillator which is investigated in [59]:

$$\begin{aligned} \dot{x} &= y, \\ \dot{u} &= -x + y\cos(x). \end{aligned} \tag{1}$$

Inspired by system (1), we introduce the following 2D new and simple conservative nonlinear system:

$$\begin{aligned} \dot{x} &= -y, \\ \dot{y} &= \sin(ax) + k\sin(bx). \end{aligned} \tag{2}$$

In this paper, the most following elegant [37] set of parameters ($a = (\sqrt{2}/2)$, $b = (1/20)$, and $k = 2$) are used in the detail investigation of the new conservative megastable system in order to uncover exciting and interesting dynamical behaviors. The equilibrium point or fixed points of system (2) can be calculated by equating to zero the right hand side of system (2). Therefore, we obtained the following transcendental equation:

$$\phi(x) = \sin(ax) + k\sin(bx) = 0. \tag{3}$$

The graphical representation of function $\phi(\mathrm{x})$ in the interval [−140, 140] is shown in Figure 1. According to this graph, one can see that there are infinite values of x which satisfy equation (3) when the range of the graphical representation is increased. Therefore, the new conservative system (2) has infinite fixed points, that is, $P_i(x_i, 0)$ with $(i = 1, 2, 3, \ldots, \infty)$.

The Jacobian matrix for this system in any equilibrium points is

$$\begin{aligned} J &= \begin{pmatrix} 0 & -1 \\ -a\cos(a\tilde{x}) + kb\cos(b\tilde{x}) & 0 \end{pmatrix} \\ &\cdot (x, y) \underset{\longrightarrow}{=} (\tilde{x}, 0)\begin{pmatrix} 0 & -1 \\ -a\cos(a\tilde{x}) + kb\cos(b\tilde{x}) & 0 \end{pmatrix}. \end{aligned} \tag{4}$$

Then, the eigenvalues can be calculated accordingly as

Table 1: Categorization of 2D chaotic megastable systems with number of terms and many equilibria.

No.	Types of 2D megastable system	Number of terms	Shape of equilibria	Reference of papers
1	2D dissipative system	Three	Infinite of equilibria	[41–43, 45]
2	2D dissipative system	Three	One equilibrium point	[26]
3	2D dissipative system	Three	One equilibrium point	[38]
4	2D dissipative system	Four	Infinite of equilibria	[44]
5	2D dissipative system	Five	One equilibrium point	[39]
6	2D dissipative & conservative	Six	None	[40]
7	**2D conservative system**	**Three**	**Infinite of hyperbolic and nonhyperbolic equilibria**	**This work**

Table 2: Categorization of reported conservative chaotic systems with various characteristics.

No.	Types of conservative systems	Nature/name of system	Multistability	Megastability	Reference of papers
1	3D system	Dissipative and conservative	Yes—coexistence of two different dynamical behaviors	None	[52–54]
2	3D system	Nose-hoover	None	None	[37]
3	3D system	Other conservative systems	None	None	[55, 56]
4	4D system	Other conservative system	None	None	[57]
5	4D system	Nonhyperbolic equilibria	Yes—coexistence of two different attractors	None	[58]
6	**2D system**	**Infinite of hyperbolic and nonhyperbolic equilibria**	**Yes—infinite attractors**	**Yes—coexistence of infinite number of nested attractors**	**This work**

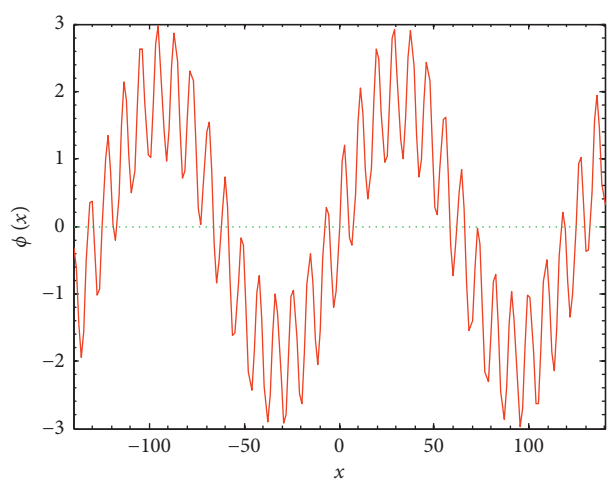

Figure 1: Graphical representation of the function $\phi(x)$ showing some views of the different fixed points of system (1) in the range $x \in [-140, 140]$.

$$|\lambda I - J| = 0 \longrightarrow \begin{vmatrix} \lambda & -1 \\ -a\cos(a\tilde{x}) + kb\cos(b\tilde{x}) & \lambda \end{vmatrix} = 0 \longrightarrow \lambda^2 + a\cos(a\tilde{x}) - kb\cos(b\tilde{x}) = 0, \quad \lambda_{1,2} = \mp\sqrt{kb\cos(b\tilde{x}) - a\cos(a\tilde{x})}. \tag{5}$$

For $kb\cos(b\tilde{x}) - a\cos(a\tilde{x}) > 0$, system (2) has infinite hyperbolic equilibria:

$$\lambda_{1,2} = \mp\sqrt{kb\cos(b\tilde{x}) - a\cos(a\tilde{x})}. \tag{5a}$$

For $kb\cos(b\tilde{x}) - a\cos(a\tilde{x}) < 0$, system (2) has infinite nonhyperbolic equilibria:

$$\lambda_{1,2} = \mp i\sqrt{kb\cos(b\tilde{x}) - a\cos(a\tilde{x})}. \tag{5b}$$

One can observe that the eigenvalues of the characteristic equation strongly depend on the fixed points $P_i(\tilde{x}, 0)$. Table 3 shows an example of the two eigenvalues of equation (5) for some equilibrium points, that is, P_1, P_2, P_3, P_4, P_5, and P_6. Based on the analysis provided in Table 3, we concluded that the points P_1, P_2, and P_4 are examples of

hyperbolic fixed points, while P_3, P_5, and P_6 are examples of nonhyperbolic fixed points. Using the previous parameter set, we carried out the numerical calculation of system (2). Some interesting and rare trajectories in this system are detected (see Figure 2). In particular, Figure 2 represents a plot of fourteen coexisting nested limit cycles in system (2). Remember that they are just an example from the infinite set of nested limit cycles around the x-axis and can be obtained under other proper initial conditions.

3. Conservative Nature of the New Oscillator

3.1. Conservative Using Divergence Property. The nonlinear dynamical system (2) can be expressed in vector notation as

$$\dot{Y} = f(Y) = \begin{cases} f_1(x, y), \\ f_2(x, y), \end{cases} \tag{6}$$

where $Y \in R^2$ is a state vector and $f(Y)$ is the smooth function given by

$$\begin{cases} f_1(x, y) = -y, \\ f_2(x, y) = \sin(ax) + k\sin(bx). \end{cases} \tag{7}$$

The divergence of the vector field $(\operatorname{div}(f) = \nabla \cdot f)$ for nonlinear system (6) can be calculated as

$$\operatorname{div}(f) = \nabla \cdot f = \frac{\partial f_1}{\partial x} + \frac{\partial f_2}{\partial y}. \tag{8}$$

However, system (2) is dissipative if $\nabla \cdot f < 0$. Otherwise, system (2) is conservative.

Thus, the divergence of system (2) can be easily obtained using (8):

$$\operatorname{div}(f) = \nabla \cdot f = \frac{\partial y}{\partial x} + \frac{\partial(\sin(ax) + k\sin(bx))}{\partial y} = 0. \tag{9}$$

As a result, the megastable system (2) has a conservative nature.

Next, suppose that system (2) is expressed as $\dot{X} = h(X)$. Let Ω be any space in R^2 with a smooth boundary/surface and also $\phi_f(\Omega) = \Omega(t)$, where ϕ_f is the flow of $h(X)$. Also, consider the volume element $V(t)$ of $\Omega(t)$ in the phase space. The volume element into a new smooth boundary $\Omega(t + \mathrm{d}t)$ in an infinitesimal time $\mathrm{d}t$ is given by $V(t + \mathrm{d}t)$ and can be obtained accordingly as [60]

$$V(t + \mathrm{d}t) = V(t) + \int (h \cdot n\mathrm{d}t)\mathrm{d}S, \tag{10}$$

where S represents the area of the smooth boundary and n is the outward normal apply on the surface Ω. It is clear from (10) that

$$\frac{\mathrm{d}V}{\mathrm{d}t} = \dot{V}(t) = \frac{V(t + \mathrm{d}t) - V(t)}{\mathrm{d}t} = \int_{\Omega} (h \cdot n)\mathrm{d}S. \tag{11}$$

Thus, by using the Ostrogradsky theorem (i.e., divergence theorem) in (11), we get

Table 3: Six examples of equilibrium points P and their corresponding eigenvalues for parameters $a = (\sqrt{2}/2)$, $b = (1/20)$, and $k = 2.0$.

Equilibrium points P_i	Eigenvalues $\lambda_{1,2}$	Hyperbolic or nonhyperbolic
$P_1(0, 0)$	$\lambda_{1,2} = \pm 0.7791$	Hyperbolic
$P_2(-7.6866, 0)$	$\lambda_{1,2} = \pm 0.6124$	Hyperbolic
$P_3(58.4009, 0)$	$\lambda_{1,2} = \pm 0.7332i$	Nonhyperbolic
$P_4(72.9614, 0)$	$\lambda_{1,2} = \pm 0.5086$	Hyperbolic
$P_5(-5.2078, 0)$	$\lambda_{1,2} = \pm 0.8383i$	Nonhyperbolic
$P_6(-198.2219, 0)$	$\lambda_{1,2} = \pm 0.4035i$	Nonhyperbolic

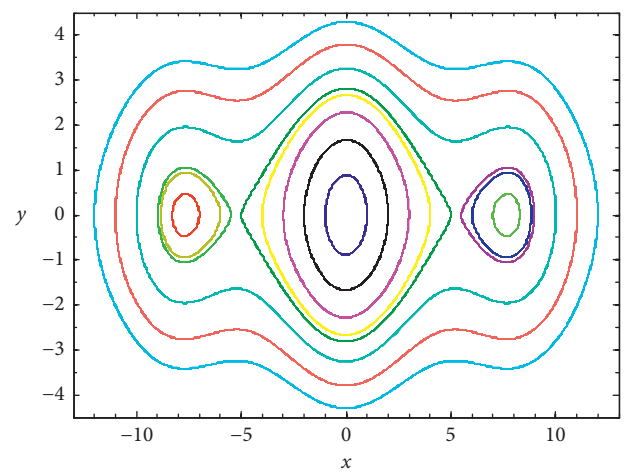

Figure 2: Fourteen examples of limit cycles of system (2) for initial conditions (1, 0), (2, 0), (3, 0), (4, 0), (5, 0), (± 5.5, 0), (± 6, 0), (± 7, 0), (10, 0), (11, 0), and (12, 0).

$$\frac{\mathrm{d}V}{\mathrm{d}t} = \dot{V}(t) = \oiiint_V (\Delta \cdot h)\mathrm{d}V, \tag{12}$$

where $(\Delta \cdot h)$ is the divergence of h.

Since the divergence of system (2) is zero, we can write (11) as

$$\frac{\mathrm{d}V}{\mathrm{d}t} = \dot{V}(t) = 0. \tag{13}$$

From (13), we get

$$V(t) = V(0). \tag{14}$$

It is observed from (14) that the volume in the phase space of system (2) is a constant. So, system (2) has conservative behavior.

3.2. Conservative Nature Using Hamiltonian-Based Analysis. The electrical activity of the systems is related to their energy modification [44]. Recently, the Hamiltonian energy function-based method is employed for the study of chaotic systems. Some technics to find the Hamilton energy function in chaotic systems have been presented [61]. In particular, a general procedure for investigation of generalized

Hamiltonian realization of an n-dimensional autonomous dynamical system is reported [62].

Consider the following dynamical system:

$$\dot{x} = F(x), \tag{15}$$

where $x \in R^n$ and $F: U \longrightarrow R^n$ is a smooth function so that $U \subseteq R^n$. The dynamical system (15) can be written in a generalized Hamiltonian form [63, 64] as

$$\dot{x} = M(x)\nabla H, \tag{16}$$

where $M(x)$ is the local structure matrix and ∇H is the gradient vector of a smooth energy function $H(x)$. For Hamiltonian system, $M(x)$ is a skew-symmetric matrix which satisfies the Jacobian identity. Otherwise, where $M(x)$ is not skew-symmetric, the system is generalized Hamiltonian. However, for a generalized Hamiltonian system, $M(x)$ can be divided as a sum of one skew-symmetric matrix $J(x)$ plus one symmetric matrix $R(x)$. Therefore, equation (16) can be written accordingly as

$$\dot{x} = (J(x) + R(x))\nabla H. \tag{17}$$

As a result, $J(x)$ and $R(x)$ can be obtained as follows:

$$\begin{aligned} \dot{H} &= \frac{\mathrm{d}H}{\mathrm{d}t} = \nabla H^T R(x)\nabla H, \\ \nabla H^T J(x)\nabla H &= 0. \end{aligned} \tag{18}$$

According to Helmholtz's theorem, system (15) can be regarded as the vector field to discuss the energy problems and can be decomposed into the rotational tensor $F_c(x)$ and gradient vector $F_d(x)$, that is,

$$F(x) = F_c(x) + F_d(x), \tag{19}$$

thus

$$\begin{aligned} \dot{H} &= \nabla H^T F_d(x), \\ J(x)\nabla H^T &= F_c(x). \end{aligned} \tag{20}$$

For $J(x)$ to be a skew-symmetric matrix,

$$\nabla H^T F_c(x) = 0, \tag{21}$$

where $H(x)$ is the Hamiltonian function and ∇H is the gradient vector of $H(x)$ defined by

$$\nabla H = \left(\frac{\partial H}{\partial x}, \frac{\partial H}{\partial y}\right)^T. \tag{22}$$

The new 2D conservative autonomous system (2) can be rewritten as

$$\begin{pmatrix} \dot{x} \\ \dot{y} \end{pmatrix} = \begin{Bmatrix} -y \\ \sin(ax) + k\sin(bx) \end{Bmatrix} + \begin{Bmatrix} 0 \\ 0 \end{Bmatrix}, \tag{23}$$

where

$$\begin{aligned} F_c(x) &= \begin{pmatrix} -y \\ \sin(ax) + k\sin(bx) \end{pmatrix}, \\ F_d(x) &= \begin{pmatrix} 0 \\ 0 \end{pmatrix}. \end{aligned} \tag{24}$$

Since $F_d(x) = (0,0)^T$, it means that there is no dissipation term in system (2) and trajectories are corresponding to the unique conservative field $F_c(x)$. That is, when the trajectories begin from an isosurface of the constant Hamilton energy $H(x)$, they cannot escape from the isosurface [57, 58].

According to (22), the Hamilton energy function $H(x, y)$ will satisfy the partial differential equation given by

$$y\frac{\partial H}{\partial x} - (\sin(ax) + k\sin(bx))\frac{\partial H}{\partial y} = 0. \tag{25}$$

So, a general solution of (25) can be approached by

$$H(x, y, a, b, k) = \frac{1}{2}y^2 - \frac{1}{a}\cos(ax) - \frac{k}{b}\cos(bx). \tag{26}$$

The time derivative of (26) can be calculated by

$$\begin{aligned} \dot{H}(x, y, a, b, k) &= y.\dot{y} + (\sin(ax) + k\sin(bx)) \cdot \dot{x} \\ &= y(\sin(ax) + k\sin(bx)) - y(\sin(ax) + k\sin(bx)) \\ &= 0 \\ &= \nabla H^T f_d(x). \end{aligned} \tag{27}$$

Since the time derivative of Hamiltonian energy of system (2) is zero, this Hamilton energy function is invariable. This justifies the conservative nature of the new system (2). Thus, the conservative property of system (2) is validated using theoretical measures.

4. The Forced Chaotic Oscillator

Like in the van der Pol equation, a temporally periodic forcing term $(A\sin(\omega t))$ can be added to nonlinear system (2), and thus we introduced the following system to describe the forced version of (2):

$$\begin{aligned} \dot{x} &= -y, \\ \dot{y} &= \sin(ax) + k\sin(bx) + A\sin(wt). \end{aligned} \tag{28}$$

In the following sections, the dynamical analysis of system (28) is discussed using various numerical tools including two-parameter Lyapunov exponents, Lyapunov spectrum plots, and phase trajectories. Here, the main objective is finding possible domains of chaotic attractors in (28). In this regard, several combinations of (A, w, k) can be used to obtain chaos. For more simplicity, we choose $w = 0.7$, and we consider the same set of system parameter a, b as in the previous section. Therefore, the dynamics of the new system (28) is investigated in terms of (A, k).

4.1. Two-Parameter Lyapunov Exponent Analysis and Multistability. The dynamical regions of the simple Hamiltonian megastable system are drawn in this part by means of two-parameter Lyapunov exponent analysis when varying the control parameter A and k in the appropriate domain. However, the global dynamic behaviors of the system can be well quantified exploiting two-parameter Lyapunov exponents by adjusting simultaneously these two last parameters of the 2D system (28) through the establishment of appropriate colorful diagrams. The obtained colorful diagrams are produced by the Lyapunov exponent spectrum on a grid of 500×500 values of the two control space parameters (i.e., A and k). The main advantage of the two-parameter Lyapunov exponent is that the complexity of the system can be directly analyzed on the variation of two parameters, which offers a major advantage over the traditional exponent which is defined on a single parameter. To properly obtain this result, system (28) is numerically solved using the standard fourth-order Runge–Kutta integration method with a fixed step size equal to 4×10^{-3}. We also used 26×10^4 steps to compute the Lyapunov exponent (LE). Figure 3 shows the two-parameter Lyapunov exponents in the parameter space (A, k) using two different initial conditions. Periodic and quasiperiodic regions are indicated by blue and cyan colors, respectively, while chaotic oscillations are materialized by yellowish-reddish color. The graphs are obtained by increasing both control parameters. From these graphs, one can observe the regions of coexisting behaviors (i.e., hysteretic dynamics) characterized by the presence of different colors in the map. To better highlight the presence of multiple coexisting attractors, we have plotted the trajectories showing different coexisting strange attractors of system (28) for $A = 0.58$ and $k = 2$ as shown in Figure 4.

4.2. Infinite Number of Coexisting Nested Strange Attractors. For more simplicity, we set $k = 2$ and consider A as a control parameter of system (28). Figure 5 shows the Lyapunov spectrum plots when parameter A is varied from 0 to 1.2 with initial conditions $(1, 0)$. One can note from this diagram that the forced version of new system (2) presents a very large range of chaotic dynamic provided that in the region $0.12 < A \leq 1.2$, $\lambda_1 > 0$, $\lambda_2 = 0$, and $\lambda_3 < 0$. However, the conservative nature of the new two-dimensional megastable system is also appreciated because $\sum_{i=1}^{3} \lambda_i = 0$ [55, 56, 65]. That is, the maximum value of LE (λ_1) and the minimum value (λ_3) are symmetric with respect to λ_2. When ICs are $(1, 0)$ and $A = 0.58$, the corresponding LEs are $\lambda_1 = 0.0943$, $\lambda_2 = 0.000$, and $\lambda_3 = -0.0943$.

However, $\sum_{i=1}^{2} \lambda_i = \lambda_1 > 0$ and $\sum_{i=1}^{3} \lambda_i = \lambda_1 + \lambda_2 = 0$. The Kaplan–Yorke dimension (Lyapunov dimension) is defined as

$$D_{KY} = D + \frac{\sum_{i=1}^{D} \lambda_D}{\left|\lambda_{D+1}\right|}, \tag{29}$$

where D is the largest integer satisfying $\sum_{i=1}^{D} \lambda_D \geq 0$ and $\sum_{i=1}^{D+1} \lambda_D < 0$. Thus, $D_{KY} = 3$ provided that $\sum_{i=1}^{3} \lambda_i = \sum_{i=1}^{D} \lambda_i = 0$.

Furthermore, using four different initial conditions, the nested coexisting bifurcation diagrams of system (28) are plotted and superimposed as shown in Figure 6. The graphs represent the plot of local maximal values of y in terms of the control parameter A that is varied (i.e., increased) in the range $0 < A \leq 1.2$. The presence of four different coexisting data in Figure 6 further confirms the complicated dynamical behaviors observed in this work. As a result, the presence of infinite number of nested attractors for A = 1.2 is depicted in Figure 7(a) and the zoom (i.e., attractors in the red box of Figure 7(a)) is shown in Figure 7(b). Note that these plots are just examples in an infinite number of stable states around the x-axis, which could be found under other proper initial conditions.

5. Circuit Implementation

In this part of our work, an analog circuit is constructed and used to make a comparison between the theoretical/numerical results obtained previously and the experimental results. The circuit implementation defines the analog circuit of our model, which confirms a possibility of laboratory measurement. Unlike other simulation software, PSpice remains the best software by its capacity to integrate the transient time. The circuit diagram that allows us to perform the various simulations in the PSpice software is presented in Figure 8. This electronic implementation of the model is very singular because the model is built based only on linear and trigonometric terms. The circuit of the new system is designed using two capacitors (C_1, C_2) and ten resistors $(R_1, \ldots, R_{10})$ including five op-amps TL082CD. In addition, it uses two sine blocs, one AC source, and a symmetric power supply. The circuit equation using Kirchhoff's electrical circuit laws can be obtained as

$$\begin{cases} C_1 \dfrac{\mathrm{d}X}{\mathrm{d}t} = -\dfrac{1}{R_1} Y, \\ \\ C_2 \dfrac{\mathrm{d}Y}{\mathrm{d}t} = \dfrac{1}{R_6} \sin\left(\dfrac{R_3}{R_2} X\right) + \dfrac{1}{R_7} \sin\left(\dfrac{R_5}{R_4} X\right) + \dfrac{V_{e\max}}{R_8} \sin(Wt). \end{cases} \tag{30}$$

Set $C_1 = C_2 = C = 10\,\mathrm{nF}$, $V_{e\max} = 1\,\mathrm{V}$, and $R = R_i = 10\,\mathrm{K\Omega}$ except R_2, R_5, R_{10}, R_{12}, and R_{13}; adopt the rescale of time $t = \tau RC$ and variables $X = 10V \times x$ and $Y = 1V \times y$.

System (30) is the same as the introduced system (28) with the following expression of parameters:

$R_1 = 10R = 100K\Omega$, $R_2 = (R/10a) = 1.414\,\mathrm{K\Omega}$, $R_4 = (R/10b) = 20\,\mathrm{K\Omega}$, $R_7 = (R/K) = 5\,\mathrm{K\Omega}$, $W = w_0 w = 7000$, and $R_8 = (V_{e\max} R/A) = 50\,\mathrm{K\Omega}$ with $w_0 = (1/\mathrm{RC})$.

The dynamics of the circuit provided in Figure 8 is simulated in PSpice as provided in Figure 9. This obtained result agrees with the one obtained based on Pascal simulation. From this figure, it can be seen that some of the

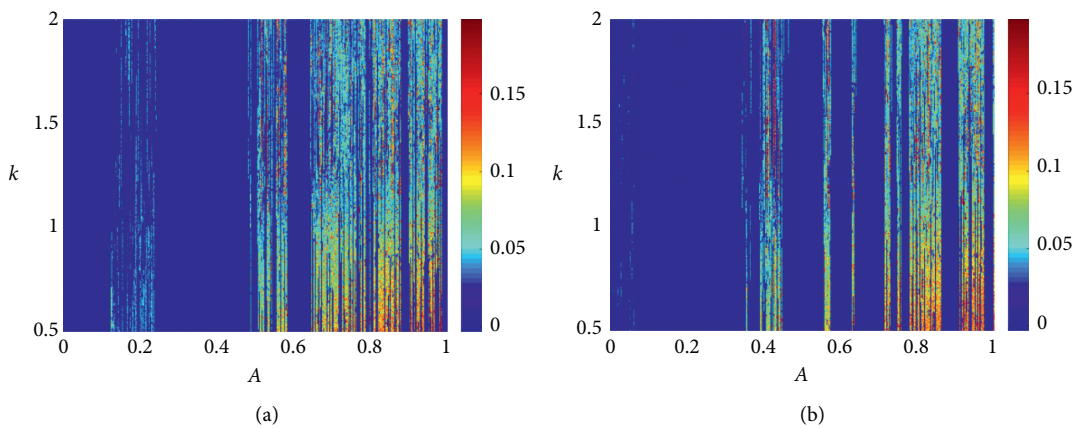

Figure 3: Coexisting of two-parameter sweep diagrams plotted in the same range of parameters with just two different initial conditions $(30, 0.2)$ and $(1, 0.2)$. The coexisting solution regions are synthesized by the simultaneous appearance of different colors on figures for the same range of parameters. The rest of the system parameters are fixed as in the text.

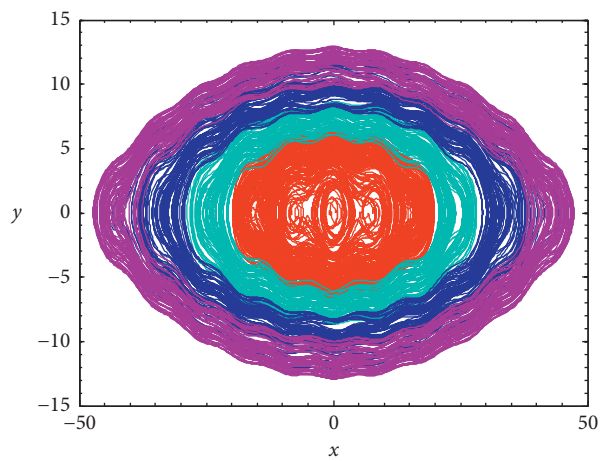

Figure 4: Trajectories showing different coexisting strange attractors of system (28) for $A = 0.58$. Each trajectory is for a duration of 1200 seconds.

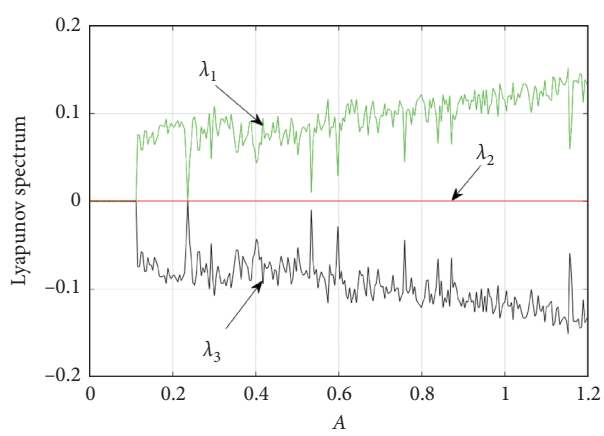

Figure 5: Lyapunov exponent spectrum for system (28) versus forcing amplitude A when $w = 0.7$. This graph is plotted with initial condition (1, 0).

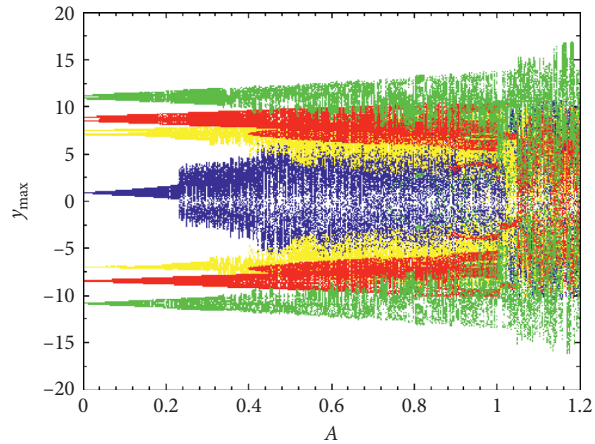

FIGURE 6: Nested bifurcation diagrams of local maxima of "y" versus forcing amplitude A in system (28) with $w = 0.7$. Four sets of data are superimposed with initial conditions blue (1, 0.2), black (25, 0.2), red (30, 0.2), and green (43, 0.2) without reinitiating.

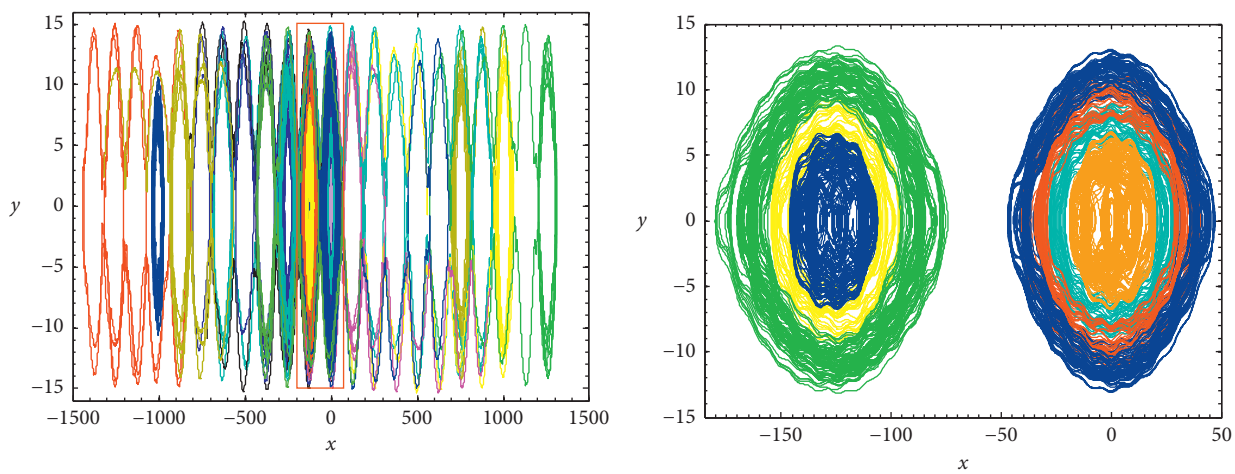

(a) (b)

FIGURE 7: (a) Trajectories in system (28) for A = 1.2, with 75 initial conditions located on the x-axis (from x = −150 to y = 150 with steps equal to 4). Each trajectory is plotted for 1200 seconds. (b) The enlarged version of the selected window in (a) (for interpretation of the references to color in this figure legend, the reader is referred to the web version of this article).

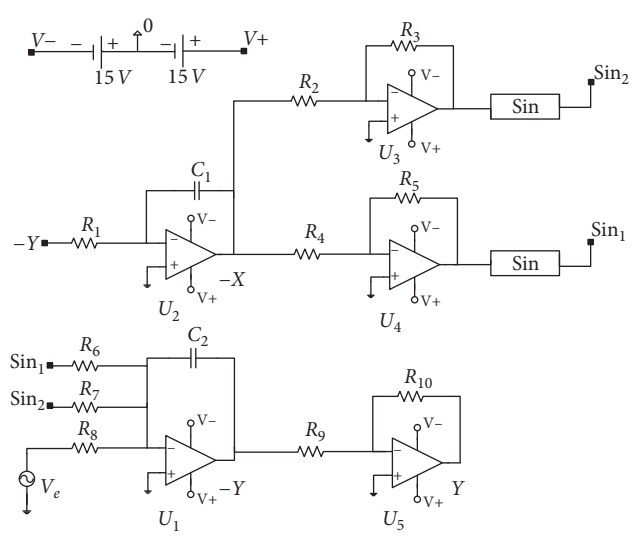

FIGURE 8: Analog computer of the new Hamiltonian megastable oscillator.

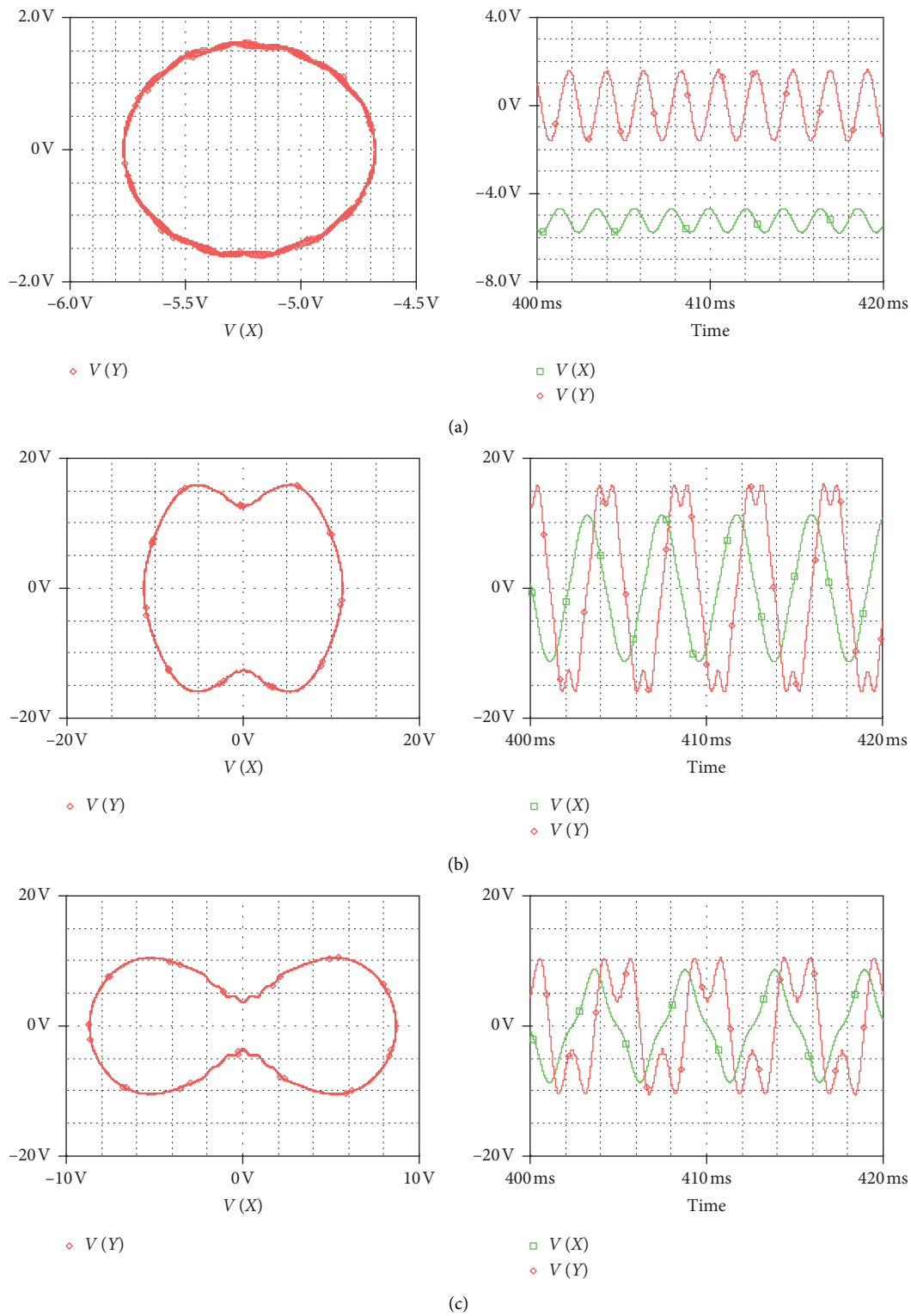

FIGURE 9: Some coexisting attractors obtained from the new megastable oscillator for $R_8 = 50\,\mathrm{K\Omega}$ ($A = 0.2$) with initial conditions $(5\,\mathrm{V}, 1\,\mathrm{V})$, $(10\,\mathrm{V}, 1\,\mathrm{V})$, and $(8\,\mathrm{V}, 1\,\mathrm{V})$, respectively.

coexisting attractors of the new megastable oscillator have been captured and support the fact that the obtained results were not artifacts.

6. Concluding Remark

This paper was focused on the dynamical analysis of the simple 2D autonomous system with infinite of hyperbolic and nonhyperbolic equilibria reported to date. The investigations of the Hamiltonian and dissipation properties of the model reveal that it is conservative and displays the coexistence of a large number of stable states. Equally, it is demonstrated under the presence of a sinusoidal excitation that the proposed model exhibits the striking phenomenon of megastability characterized by the coexistence of an infinite number of countable stable states. Finally, the electronic implementation of the introduced model has been provided using PSPice simulations to further support our results. In the future, it would be interesting to carry out the analytical methods which can predict megastability behaviors in a nonlinear system and address the megastable system-based secure communication.

Data Availability

The data used to support the findings of this study are included within the article.

Conflicts of Interest

The authors declare no conflicts of interest.

References

[1] A. Bayani, K. Rajagopal, A. J. M. Khalaf, S. Jafari, G. D. Leutcho, and J. Kengne, "Dynamical analysis of a new multistable chaotic system with hidden attractor: antimonotonicity, coexisting multiple attractors, and offset boosting," *Physics Letters A*, vol. 383, no. 13, pp. 1450–1456, 2019.

[2] T. Fonzin Fozin, P. Megavarna Ezhilarasu, Z. Njitacke Tabekoueng et al., "On the dynamics of a simplified canonical Chua's oscillator with smooth hyperbolic sine nonlinearity: hyperchaos, multistability and multistability control," *Chaos: An Interdisciplinary Journal of Nonlinear Science*, vol. 29, no. 11, Article ID 113105, 2019.

[3] T. F. Fonzin, J. Kengne, and F. Pelap, "Dynamical analysis and multistability in autonomous hyperchaotic oscillator with experimental verification," *Nonlinear Dynamics*, vol. 93, pp. 653–669, 2018.

[4] S. He, K. Sun, X. Mei, B. Yan, and S. Xu, "Numerical analysis of a fractional-order chaotic system based on conformable fractional-order derivative," *The European Physical Journal Plus*, vol. 132, pp. 1–11, 2017.

[5] Z. T. Njitacke and J. Kengne, "Complex dynamics of a 4D Hopfield neural networks (HNNs) with a nonlinear synaptic weight: coexistence of multiple attractors and remerging Feigenbaum trees," *AEU—International Journal of Electronics and Communications*, vol. 93, pp. 242–252, 2018.

[6] Z. Wei, Y. Li, B. Sang, Y. Liu, and W. Zhang, "Complex dynamical behaviors in a 3D simple chaotic flow with 3D stable or 3D unstable manifolds of a single equilibrium," *International Journal of Bifurcation and Chaos*, vol. 29, no. 7, Article ID 1950095, 2019.

[7] Z. Wei, I. Moroz, J. Sprott, A. Akgul, and W. Zhang, "Hidden hyperchaos and electronic circuit application in a 5D self-exciting homopolar disc dynamo," *Chaos: An Interdisciplinary Journal of Nonlinear Science*, vol. 27, Article ID 033101, 2017.

[8] V.-T. Pham, A. Akgul, C. Volos, S. Jafari, and T. Kapitaniak, "Dynamics and circuit realization of a no-equilibrium chaotic system with a boostable variable," *AEU—International Journal of Electronics and Communications*, vol. 78, pp. 134–140, 2017.

[9] D. I. Martinez, J. J. De Rubio, T. M. Vargas et al., "Stabilization of robots with a regulator containing the sigmoid mapping," *IEEE Access*, vol. 8, pp. 89479–89488, 2020.

[10] J. D. J. Rubio, D. I. Martinez, V. Garcia et al., "The perturbations estimation in two gas plants," *IEEE Access*, vol. 8, pp. 83081–83091, 2020.

[11] J. D. J. Rubio, G. Ochoa, D. Mujica-Vargas et al., "Structure regulator for the perturbations attenuation in a quadrotor," *IEEE Access*, vol. 7, pp. 138244–138252, 2019.

[12] C. Aguilar-Ibanez and M. S. Suarez-Castanon, "A trajectory planning based controller to regulate an uncertain 3D overhead crane system," *International Journal of Applied Mathematics and Computer Science*, vol. 29, no. 4, pp. 693–702, 2019.

[13] B. Bao, Q. Yang, D. Zhu, Y. Zhang, Q. Xu, and M. Chen, "Initial-induced coexisting and synchronous firing activities in memristor synapse-coupled Morris–Lecar bi-neuron network," *Nonlinear Dynamics*, vol. 99, no. 3, pp. 2339–2354, 2020.

[14] H. Bao, N. Wang, B. Bao, M. Chen, P. Jin, and G. Wang, "Initial condition-dependent dynamics and transient period in memristor-based hypogenetic jerk system with four line equilibria," *Communications in Nonlinear Science and Numerical Simulation*, vol. 57, pp. 264–275, 2018.

[15] B. Bo-Cheng, L. Zhong, and X. Jian-Ping, "Transient chaos in smooth memristor oscillator," *Chinese Physics B*, vol. 19, Article ID 030510, 2010.

[16] J. O. Escobedo-Alva, E. C. Garcia-Estrada, L. A. Páramo-Carranza, J. A. Meda-Campaña, and R. Tapia-Herrera, "Theoretical application of a hybrid observer on altitude tracking of quadrotor losing GPS signal," *IEEE Access*, vol. 6, pp. 76900–76908, 2018.

[17] Q. Lai, P. D. K. Kuate, F. Liu, and H. H.-C. Iu, "An extremely simple chaotic system with infinitely many coexisting attractors," *IEEE Transactions on Circuits and Systems II: Express Briefs*, vol. 67, no. 6, pp. 1129–1133, 2019.

[18] B. Bao, L. Xu, Z. Wu, M. Chen, and H. Wu, "Coexistence of multiple bifurcation modes in memristive diode-bridge-based canonical Chua's circuit," *International Journal of Electronics*, vol. 105, no. 7, pp. 1159–1169, 2018.

[19] G. D. Leutcho, J. Kengne, and L. K. Kengne, "Dynamical analysis of a novel autonomous 4-D hyperjerk circuit with hyperbolic sine nonlinearity: chaos, antimonotonicity and a plethora of coexisting attractors," *Chaos, Solitons & Fractals*, vol. 107, pp. 67–87, 2018.

[20] S. He, K. Sun, and Y. Peng, "Detecting chaos in fractional-order nonlinear systems using the smaller alignment index," *Physics Letters A*, vol. 383, no. 19, pp. 2267–2271, 2019.

[21] S. He, K. Sun, and H. Wang, "Dynamics and synchronization of conformable fractional-order hyperchaotic systems using the Homotopy analysis method," *Communications in Nonlinear Science and Numerical Simulation*, vol. 73, pp. 146–164, 2019.

[22] J. Ruan, K. Sun, J. Mou, S. He, and L. Zhang, "Fractional-order simplest memristor-based chaotic circuit with new derivative," *The European Physical Journal Plus*, vol. 133, no. 3, 2018.

[23] L. K. Kengne, J. Kengne, J. R. Mboupda Pone, and H. T. Kamdem Tagne, "Symmetry breaking, coexisting bubbles, multistability, and its control for a simple jerk system with hyperbolic tangent nonlinearity," *Complexity*, vol. 2020, Article ID 2340934, 24 pages, 2020.

[24] G. D. Leutcho, J. Kengne, T. Fonzin Fozin et al., "Multistability control of space magnetization in hyperjerk oscillator: a case study," *Journal of Computational and Nonlinear Dynamics*, vol. 15, no. 5, 2020.

[25] S. Vaidyanathan, I. Pehlivan, L. G. Dolvis et al., "A novel ANN-based four-dimensional two-disk hyperchaotic dynamical system, bifurcation analysis, circuit realisation and FPGA-based TRNG implementation," *International Journal of Computer Applications in Technology*, vol. 62, no. 1, pp. 20–35, 2019.

[26] J. C. Sprott, S. Jafari, A. J. M. Khalaf, and T. Kapitaniak, "Megastability: coexistence of a countable infinity of nested attractors in a periodically-forced oscillator with spatially-periodic damping," *The European Physical Journal Special Topics*, vol. 226, no. 9, pp. 1979–1985, 2017.

[27] G. D. Leutcho and J. Kengne, "A unique chaotic snap system with a smoothly adjustable symmetry and nonlinearity: chaos, offset-boosting, antimonotonicity, and coexisting multiple attractors," *Chaos, Solitons & Fractals*, vol. 113, pp. 275–293, 2018.

[28] C. Li, J. C. Sprott, W. Hu, and Y. Xu, "Infinite multistability in a self-reproducing chaotic system," *International Journal of Bifurcation and Chaos*, vol. 27, no. 10, Article ID 1750160, 2017.

[29] C. Li, J. C. Sprott, and H. Xing, "Constructing chaotic systems with conditional symmetry," *Nonlinear Dynamics*, vol. 87, no. 2, pp. 1351–1358, 2017.

[30] T. Lu, C. Li, S. Jafari, and F. Min, "Controlling coexisting attractors of conditional symmetry," *International Journal of Bifurcation and Chaos*, vol. 29, no. 14, Article ID 1950207, 2019.

[31] C. Li, J. C. Sprott, T. Kapitaniak, and T. Lu, "Infinite lattice of hyperchaotic strange attractors," *Chaos, Solitons & Fractals*, vol. 109, pp. 76–82, 2018.

[32] J. Ma, X. Wu, R. Chu, and L. Zhang, "Selection of multi-scroll attractors in Jerk circuits and their verification using Pspice," *Nonlinear Dynamics*, vol. 76, no. 4, pp. 1951–1962, 2014.

[33] S.-B. He, K.-H. Sun, and G.-X. Zhu, "Complexity analyses of multi-wing chaotic systems," *Chinese Physics B*, vol. 22, no. 5, Article ID 050506, 2013.

[34] W. K. S. Tang, G. Q. Zhong, G. Chen, and K. F. Man, "Generation of *n*-scroll attractors via sine function," *IEEE Transactions on Circuits and Systems I: Fundamental Theory and Applications*, vol. 48, no. 11, pp. 1369–1372, 2001.

[35] J. Gu, C. Li, Y. Chen, H. H. C. Iu, and T. Lei, "A conditional symmetric memristive system with infinitely many chaotic attractors," *IEEE Access*, vol. 8, pp. 12394–12401, 2020.

[36] C. Li, Y. Xu, G. Chen, Y. Liu, and J. Zheng, "Conditional symmetry: bond for attractor growing," *Nonlinear Dynamics*, vol. 95, no. 2, pp. 1245–1256, 2019.

[37] J. C. Sprott, *Elegant Chaos: Algebraically Simple Chaotic Flows*, World Scientific, Singapore, 2010.

[38] S. Jafari, K. Rajagopal, T. Hayat, A. Alsaedi, and V.-T. Pham, "Simplest megastable chaotic oscillator," *International Journal of Bifurcation and Chaos*, vol. 29, no. 13, Article ID 1950187, 2019.

[39] P. Prakash, K. Rajagopal, J. P. Singh, and B. K. Roy, "Megastability in a quasi-periodically forced system exhibiting multistability, quasi-periodic behaviour, and its analogue circuit simulation," *AEU—International Journal of Electronics and Communications*, vol. 92, pp. 111–115, 2018.

[40] K. Rajagopal, J. P. Singh, B. K. Roy, and A. Karthikeyan, "Dissipative and conservative chaotic nature of a new quasi-periodically forced oscillator with megastability," *Chinese Journal of Physics*, vol. 58, pp. 263–272, 2019.

[41] Y. Tang, H. R. Abdolmohammadi, A. J. M. Khalaf, Y. Tian, and T. Kapitaniak, "Carpet oscillator: a new megastable nonlinear oscillator with infinite islands of self-excited and hidden attractors," *Pramana*, vol. 91, p. 11, 2018.

[42] Y.-X. Tang, A. J. M. Khalaf, K. Rajagopal, V.-T. Pham, S. Jafari, and Y. Tian, "A new nonlinear oscillator with infinite number of coexisting hidden and self-excited attractors," *Chinese Physics B*, vol. 27, Article ID 040502, 2018.

[43] Z. Wang, H. R. Abdolmohammadi, F. E. Alsaadi, T. Hayat, and V.-T. Pham, "A new oscillator with infinite coexisting asymmetric attractors," *Chaos, Solitons & Fractals*, vol. 110, pp. 252–258, 2018.

[44] Z. Wang, I. I. Hamarash, P. S. Shabestari, and S. Jafari, "A new megastable oscillator with rational and irrational parameters," *International Journal of Bifurcation and Chaos*, vol. 29, no. 13, Article ID 1950176, 2019.

[45] Z. Wei, V.-T. Pham, A. J. M. Khalaf, J. Kengne, and S. Jafari, "A modified multistable chaotic oscillator," *International Journal of Bifurcation and Chaos*, vol. 28, no. 7, Article ID 1850085, 2018.

[46] G. D. Leutcho, S. Jafari, I. I. Hamarash, J. Kengne, Z. Tabekoueng Njitacke, and I. Hussain, "A new megastable nonlinear oscillator with infinite attractors," *Chaos, Solitons & Fractals*, vol. 134, Article ID 109703, 2020.

[47] G. D. Leutcho, A. J. M. Khalaf, Z. Njitacke Tabekoueng et al., "A new oscillator with mega-stability and its Hamilton energy: infinite coexisting hidden and self-excited attractors," *Chaos: An Interdisciplinary Journal of Nonlinear Science*, vol. 30, Article ID 033112, 2020.

[48] M. Tuna, A. Karthikeyan, K. Rajagopal, M. Alcin, and İ. Koyuncu, "Hyperjerk multiscroll oscillators with megastability: analysis, FPGA implementation and a novel ANN-ring-based true random number generator," *AEU—International Journal of Electronics and Communications*, vol. 112, Article ID 152941, 2019.

[49] S. Jafari, J. C. Sprott, and S. Dehghan, "Categories of conservative flows," *International Journal of Bifurcation and Chaos*, vol. 29, no. 2, Article ID 1950021, 2019.

[50] N. Wang, G. Zhang, and H. Bao, "Infinitely many coexisting conservative flows in a 4D conservative system inspired by LC circuit," *Nonlinear Dynamics*, vol. 99, pp. 3197–3216, 2020.

[51] G. Qi, J. Hu, and Z. Wang, "Modeling of a Hamiltonian conservative chaotic system and its mechanism routes from periodic to quasiperiodic, chaos and strong chaos," *Applied Mathematical Modelling*, vol. 78, pp. 350–365, 2020.

[52] A. Politi, G. L. Oppo, and R. Badii, "Coexistence of conservative and dissipative behavior in reversible dynamical systems," *Physical Review A*, vol. 33, no. 6, p. 4055, 1986.

[53] J. C. Sprott, "A dynamical system with a strange attractor and invariant tori," *Physics Letters A*, vol. 378, no. 20, pp. 1361–1363, 2014.

[54] J. C. Sprott, W. G. Hoover, and C. G. Hoover, "Heat conduction, and the lack thereof, in time-reversible dynamical systems: generalized Nosé-Hoover oscillators with a

temperature gradient," *Physical Review E*, vol. 89, Article ID 042914, 2014.

[55] G. Qi and X. Liang, "Mechanical analysis of Qi four-wing chaotic system," *Nonlinear Dynamics*, vol. 86, no. 2, pp. 1095–1106, 2016.

[56] S. Vaidyanathan and S. Pakiriswamy, "A 3-D novel conservative chaotic system and its generalized projective synchronization via adaptive control," *Journal of Engineering Science & Technology Review*, vol. 8, no. 2, pp. 52–60, 2015.

[57] S. Cang, A. Wu, Z. Wang, and Z. Chen, "Four-dimensional autonomous dynamical systems with conservative flows: two-case study," *Nonlinear Dynamics*, vol. 89, no. 4, pp. 2495–2508, 2017.

[58] J. P. Singh and B. K. Roy, "Five new 4-D autonomous conservative chaotic systems with various type of non-hyperbolic and lines of equilibria," *Chaos, Solitons & Fractals*, vol. 114, pp. 81–91, 2018.

[59] P. B. Kahn and Y. Zarmi, *Nonlinear Dynamics: Exploration through Normal Forms*, Courier Corporation, Chelmsford, MA, USA, 2014.

[60] S. H. Strogatz, *Nonlinear Dynamics and Chaos: With Applications to Physics, Biology, Chemistry, and Engineering*, CRC Press, Boca Raton, FL, USA, 2018.

[61] C. Sarasola, A. D'anjou, F. J. Torrealdea, and A. Moujahid, "Energy-like functions for some dissipative chaotic systems," *International Journal of Bifurcation and Chaos*, vol. 15, no. 8, pp. 2507–2521, 2005.

[62] J. Ma, F. Wu, W. Jin, P. Zhou, and T. Hayat, "Calculation of Hamilton energy and control of dynamical systems with different types of attractors," *Chaos: An Interdisciplinary Journal of Nonlinear Science*, vol. 27, Article ID 053108, 2017.

[63] S. Cang, A. Wu, Z. Wang, and Z. Chen, "Distinguishing Lorenz and Chen systems based upon Hamiltonian energy theory," *International Journal of Bifurcation and Chaos*, vol. 27, no. 2, Article ID 1750024, 2017.

[64] A. Xin-lei and Z. Li, "Dynamics analysis and Hamilton energy control of a generalized Lorenz system with hidden attractor," *Nonlinear Dynamics*, vol. 94, no. 4, pp. 2995–3010, 2018.

[65] E. Dong, X. Jiao, S. Du, Z. Chen, and G. Qi, "Modeling, synchronization, and FPGA implementation of Hamiltonian conservative hyperchaos," *Complexity*, vol. 2020, Article ID 4627597, 13 pages, 2020.